

RESEARCH PAPER

 OPEN ACCESS 

The African swine fever virus protease pS273R inhibits DNA sensing cGAS-STING pathway by targeting IKK ϵ

Jia Luo^{a,b,c,d}, Jiajia Zhang^{a,b,c,d}, Jinghua Ni^{a,b,c,d}, Sen Jiang^{a,b,c,d}, Nengwen Xia^{a,b,c,d}, Yiwen Guo^{a,b,c,d}, Qi Shao^{a,b,c,d}, Qi Cao^{a,b,c,d}, Wanglong Zheng^{a,b,c,d}, Nanhua Chen^{a,b,c,d}, Quan Zhang^{a,b,c,d}, Hongjun Chen^e, Qing Chen^f, Hongfei Zhu^g, François Meurens^{h,i}, and Jianzhong Zhu^{ib}^{a,b,c,d}

^aCollege Veterinary Medicine, Yangzhou University, Yangzhou, China; ^bSafety, Yangzhou University Joint International Research Laboratory of Agriculture and Agri-Product, Yangzhou, China; ^cComparative Medicine Research Institute, Yangzhou University, Yangzhou, China; ^dJiangsu Co-Innovation Center for Prevention and Control of Important Animal Infectious Diseases and Zoonoses, Yangzhou University, Yangzhou, China; ^eShanghai Veterinary Research Institute, Chinese Academy of Agriculture Sciences, Shanghai, China; ^fCollege of Bioscience and Resource Environment, Beijing University of Agriculture, Beijing, China; ^gInstitute of Animal Science, Chinese Academy of Agricultural Sciences, Beijing, China; ^hBIOEPAR, INRAE, Oniris, Nantes, France; ⁱDepartment of Veterinary Microbiology and Immunology, Western College of Veterinary Medicine, University of Saskatchewan, Saskatoon, Canada

ABSTRACT

African swine fever virus (ASFV), a large and complex cytoplasmic double-stranded DNA virus, has developed multiple strategies to evade the antiviral innate immune responses. Cytosolic DNA arising from invading ASFV is mainly detected by the cyclic GMP-AMP synthase (cGAS) and then triggers a series of innate immune responses to prevent virus invasion. However, the immune escape mechanism of ASFV remains to be fully clarified. The pS273R of ASFV is a member of the SUMO-1-specific protease family and is crucial for valid virus replication. In this study, we identified pS273R as a suppressor of cGAS-STING pathway mediated type I interferon (IFN) production by ASFV genomic open reading frame screening. The pS273R was further confirmed as an inhibitor of IFN production as well as its downstream antiviral genes in cGAS-STING pathway. Mechanistically, pS273R greatly decreased the cGAS-STING signaling by targeting IKK ϵ but not TBK1, and pS273R was found to disturb the interaction between IKK ϵ and STING through its interaction with IKK ϵ . Further, mutational analyses revealed that pS273R antagonized the cGAS-STING pathway by enzyme catalytic activity, which might affect the IKK ϵ sumoylation state required for the interaction with STING. In summary, our results revealed for the first time that pS273R acts as an obvious negative regulator of cGAS-STING pathway by targeting IKK ϵ via its enzymatic activity, which shows a new immune evasion mechanism of ASFV.

ARTICLE HISTORY

Received 9 December 2021
Revised 18 March 2022
Accepted 11 April 2022

KEYWORDS

ASFV; pS273R; cGAS; STING; IKK ϵ ; type I interferons (IFNs)

Introduction

African swine fever (ASF), a devastating disease for domestic pigs and wild boar, usually causes an acute hemorrhagic fatal disease with a mortality rate of up to 100% while being asymptomatic in the natural hosts [1,2]. Since African swine fever was initially described in Kenya in the 1920s, it has spread rapidly across many countries in sub-Saharan African, Caribbean, Eastern Europe [3]. In 2017, a large number of outbreaks of ASF occurred in Siberia near to the Russia–China border [4]. The first outbreak of ASF in China was reported on 3 August 2018 [5] where it caused unprecedented disaster for Chinese swine industry and food security due to currently unavailable vaccines in the world. Accordingly, animal slaughter and regional quarantine are the only method for the disease control.

African swine fever virus (ASFV) is a large, complex, cytoplasmic double-stranded DNA virus. It is the sole member of the *Asfarviridae* family, but also the only DNA virus transmitted by arthropod ticks, soft ticks (*Ornithodoros moubata*) [6]. ASFV is an enveloped virus with icosahedral structure inside which is composed of four concentric layers from the central nucleoid, the core shell, the inner envelope to the outside the icosahedral capsid [7]. The average diameter of the ASFV is approximately 200 nm and genomes vary in length between 170 and 193 kb which depends on the isolates. ASFV contains between 151 and 167 open reading frames (ORFs), which encode structural proteins, viral DNA replication proteins and host defense escape protein *etc* [8].

The open reading frame (ORF) S273R encodes a 31-kD protein, and the protein pS273R belongs to

CONTACT Jianzhong Zhu  jzzhu@yzu.edu.cn

 Supplemental data for this article can be accessed online at <https://doi.org/10.1080/21505594.2022.2065962>

© 2022 The Author(s). Published by Informa UK Limited, trading as Taylor & Francis Group.
This is an Open Access article distributed under the terms of the Creative Commons Attribution License (<http://creativecommons.org/licenses/by/4.0/>), which permits unrestricted use, distribution, and reproduction in any medium, provided the original work is properly cited.

the SUMO-1-specific protease family with the ability to catalyze the maturation of pp220 and pp62 polyprotein precursors into core shell matrix proteins [9]. The two significant polyproteins, pp220 and pp62, are cleaved by the pS273R protease to produce six primary structural components of the virus particle, among which p37, p34, p40, p150 derived from polyproteins pp220 and p15, p35 derived from polyproteins pp62 [10]. Therefore, the pS273R protease is of great significance for maturation and infectivity of the ASFV particle.

The innate immune system is the body's first line of defense against pathogen infection. It utilizes a variety of pattern recognition receptors (PRRs) in cells to recognize and respond to pathogen associated molecular patterns (PAMPs) [11]. Among various PRRs, cyclic GMP-AMP synthase (cGAS) is a cytosolic double-stranded DNA sensor, which senses the presence of cytoplasmic DNA and catalyzes the synthesis of the second messenger cyclic GMP-AMP 2'3'-cGAMP [12]. Then 2'3'-cGAMP binds and activates the stimulator of interferon genes protein (STING), which upon stimulation, transfers from the endoplasmic reticulum (ER) to the trans-Golgi apparatus network (TGN), during which the kinase TBK1 is recruited and auto-phosphorylated [13]. TBK1 subsequently phosphorylates the transcription factor IRF3, and then IRF3 translocates into nucleus to activate the expression of antiviral type I interferons (IFNs) [14]. The DNA sensing cGAS-STING pathway is the relevant innate immunity for ASFV, however, the immune evasion of this pathway by ASFV has not been resolved. Here, we identified the viral protein responsible for the immune evasion and characterized its mechanism of action.

Materials and methods

Cells and viruses

HEK-293T cells were cultured in Dulbecco modified Eagle medium (DMEM, Hyclone Laboratories, USA) supplemented with 100 IU/mL of penicillin plus 100 µg/mL streptomycin and 10% fetal bovine serum (FBS). Porcine alveolar macrophages (PAMs, 3D4/21) were cultured in RPMI 1640 medium (Hyclone Laboratories) which contains 100 IU/mL of penicillin plus 100 µg/mL streptomycin and 10% FBS. Cells were grown at 37°C in a 5% CO₂ humidified incubator. The Vesicular Stomatitis Virus (VSV-GFP) and Herpes Simplex Virus-1 (HSV-1-GFP) were both provided by Dr. Tony Wang in SRI International USA.

Reagents and antibodies

TRIpure Reagent for RNA extraction was purchased from Aidlab (Beijing, China). HiScript® 1st Strand cDNA Synthesis Kit, ChamQ Universal SYBR qPCR Master Mix, 2×Taq Master Mix (Dye plus), 180 kDa prestained protein marker and TransDetect Double-Luciferase Reporter Assay Kit were all from Vazyme Biotech Co., Ltd (Nanjing, China). The Golden Star T6 Super PCR mix polymerase and KOD plus neo polymerase were from Tsingke (Nanjing, China) and Toyobo (Shanghai, China), respectively. The 2×MultiF Seamless Assembly Mix was acquired from Abclonal (Wuhan, China). Restriction endonucleases *Hind* III, *Kpn* I, *EcoR* I, *EcoR* V, *Dnp* I were purchased from New England Biolabs (Beijing, China). Agonists polydA:dT and 2'3'-cGAMP were bought from InvivoGen (Hongkong, China). Forty-five base pair double-stranded DNA (45bp dsDNA, tacagatctactagtgatctatgactgatctgtacatgatctaca) was synthesized by GENEWIZ (Shouzhou, China). Lipofectamine™ 2000 were acquired from ThermoFisher Scientific (Shanghai, China). Chemical inhibitor 2-D08 was purchased from Selleck (Shanghai, China). Protein A/G Plus-Agarose was from Santa Cruz Biotechnology (Dallas, Texas, USA). Mouse anti-FLAG mAb, mouse anti-Actin mAb, mouse anti-GFP mAb were all acquired from Transgen Biotech (Beijing, China). The HRP anti-mouse IgG, HRP anti-rabbit IgG were purchased from Sangon Biotech (Shanghai, China). The rabbit anti-TBK1 (D1B4), anti-*p*-TBK1 (S172), anti-*p*-IRF3 (4D4G), anti-IRF3 (D164C), anti-HA (C29F4), anti-sumo-2/3 (18H8) were bought from Cell Signaling Technology (Danvers, MA, US). Rabbit anti-STING pAb was from ProteinTech (Wuhan, China). Rabbit anti-ISG56-pAb was homemade in our lab. Mouse anti-ASFV p30 mAb was nicely provided by Drs. Xinyu Zhang and Xilong Kang. DAPI staining solution was bought from Beyotime Biotech (Shanghai, China). Rabbit anti-mCHERRY-pAb, mouse anti-MYC mAb, Goat anti-mouse IgG H&L (Alexa Fluor®594) and goat anti-rabbit IgG H&L (Alexa Fluor®647) were purchased from Abcam (Shanghai, China).

Plasmid construction and gene mutations

The genomic ORFs of ASFV China 2018/1 (GenBank submission No: MH766894) were codon optimized, synthesized and cloned into p3×FLAG-CMV-7.1 vector using *Not* I and *Sal* I sites. The 145 sequence confirmed ORF plasmids were used for screening of modulators of porcine cGAS-STING signaling pathway by ISRE promoter assay (Supplementary Figure S1). The S273R

gene was amplified by PCR using Golden Star T6 Super PCR Mix polymerase from plasmid p3×FLAG-CMV-S273R and then was cloned into pCAGGS-HA vector using *EcoR* I and *EcoR* V sites. The critical enzyme active sites of pS273R were identified and point mutated using the mutation PCR primers designed by QuickChange Primer Design method (<https://www.agilent.com>) (Supplementary Table S1). The mutation PCR was performed with KOD plus neo polymerase and pCAGGS-S273R-HA as the template. The PCR products were transformed into competent DMT *E. coli* after *Dpn* I digestion, and the resultant mutants were sequence confirmed. Truncated mutants of the pS273R, including pS273R (Δ 1–20) and pS273R (Δ 256–273) were obtained by PCR amplification and cloning into pCAGGS-HA using 2×MultiF Seamless Assembly Mix polymerase. Porcine cGAS, STING, IKK ϵ , IKK β , IRF3 and NF- κ B p65 plasmids were constructed and characterized as we reported [15]; human TBK1, IKK ϵ , IRF3-5D plasmids were preserved in our lab. The 3×FLAG-pCMV-sumo-1, 2, and 3 plasmids were all purchased from MiaoLingBio Company (Wuhan, China).

Promoter driven luciferase reporter gene assay

293T cells grown in 96-well plates ($3\text{--}4 \times 10^4$ cells/well) were co-transfected by Lipofectamine 2000 with reporter plasmids, ISRE-luc, IFN β -luc or ELAM (NF- κ B)-firefly luciferase (Fluc) (10 ng/well) plus *Renilla* luciferase (Rluc) reporter (0.2 ng/well), with or without the indicated porcine cGAS and STING plasmids as well as porcine S273R or vector control (10–20 ng/well). The total DNA amount for transfection was normalized with control vectors to 50 ng for each well. PAMs grown in 96-well plates were similarly transfected using the Lipofectamine 2000. At 24 h post transfection, cells were harvested and dual-luciferase assays were sequentially performed using the TransDetect Double-Luciferase Reporter Assay Kit. The fold changes were calculated relative to control samples after normalization of Fluc by Rluc.

Quantitative real-time PCR

Total RNA was extracted from 293T or PAMs in 24-well plates ($2\text{--}4 \times 10^5$ cells/well) with TRIpure Reagent, and cDNA synthesis was performed using HiScript[®] 1st Strand cDNA Synthesis Kit (+gDNA wiper). The quantitative PCR was then performed with ChamQ Universal SYBR qPCR Master Mix using StepOne Plus equipment (Applied Biosystems) to measure the target gene expressions. The qPCR program is

denaturing at 95°C for 30 s followed by 40 cycles of 95°C for 10 s and 60°C for 30 s. The qPCR primers for hIFN β , hISG56, hISG60, hIL8, hRPL32, pIFN β , pISG56, pIL8, p β -actin, HSV-1 gB, VSV Glycoprotein, ASFV S273R and B646L are shown in Supplementary Table S2.

Flow cytometry, virus TCID50 and plaque assay

PAMs in 6-well plate (8×10^5 cells/well) were transfected by Lipofectamine 2000 with porcine S273R expressing plasmids or vector control (1 μ g/well). About 24 h post-transfection, the transfected cells were infected or not with VSV-GFP (0.001 MOI) or HSV-GFP (0.01 MOI). After infection, the cells were harvested by trypsin digestion and washed 3× with PBS. The levels of GFP virus replication were analyzed by flow cytometry of the cell suspensions.

The supernatants of virus-infected PAMs were collected and tenfold serially diluted in DMEM medium with each dilution four to eight replications. The diluted supernatants were then used to infect Vero cells in 96-well plates for 2 h. The cells were then cultured in DMEM containing 2% FBS and grown at 37°C for 1 day (for VSV) or 2 day for (HSV-1). The cytopathic effects (CPEs) were counted and TCID50 was calculated with Reed-Muench method.

Vero cells seeded into 12-well plates and grown into monolayer were infected by the tenfold serially diluted cell supernatants from VSV infected cells for 2 h. Then, the infected cells were washed with PBS and overlaid by immobilizing medium of 1:1 mixture of warmed 2×DMEM with 4% FBS and a stock solution of heated 1.6% low melting agarose. Two days later, the immobilizing medium were discarded by tipping and cells were fixed and stained with crystal violet cell colony staining solution for 1 h at room temperature. After staining, cells were washed with tap water until the clear plaques appeared. The plaques were counted and photos were taken.

Co-immunoprecipitation and Western blot analysis

For Co-immunoprecipitation, 293T cells in 6-well plate (8×10^5 cells/well) were transfected for 48 h, and then cells were harvested and lysed in 500 μ L RIPA buffer (50 mM Tris pH 7.2, 150 mM NaCl, 1% sodium deoxycholate, 1% Triton X-100) with protease inhibitors on ice for 30 min followed by centrifugation. The 50 μ L cell lysate was saved as input controls and the remained were incubated with indicated antibodies overnight at 4 °C, and then 30 μ L 50% protein A/G bead solution was added for another 2 h. Later, the beads were thoroughly

washed five times with RIPA and boiled in 40 μ L 2 \times SDS sample buffer to obtain the elution which subjected to Western blotting. The elution samples together with input controls were boiled at 100 $^{\circ}$ C for 5–10 min, separated by 6–10% SDS-polyacrylamide gels, and transferred to PVDF membranes. Membranes were then blocked using 5% nonfat dry milk Tris-buffered saline, with 0.1% Tween-20 (TBST) at room temperature (RT) for 2 h. Next the membranes were sequentially incubated with primary antibodies overnight at 4 $^{\circ}$ C and HRP-conjugated goat anti-mouse or anti-rabbit IgG for 1 h at RT. Protein signals was visualized and captured by Western blot imaging system (Tanon, Shanghai, China).

Confocal fluorescence microscopy

PAMs grown on coverslip in 24-well plates (2×10^5 cells/well) were co-transfected by Lipofectamine 2000 with the combinations of STING-GFP, IKK ϵ -MYC, IRF3-GFP, p65-GFP and S273R. About 24 h post transfection, the cells were fixed with 4% paraformaldehyde at RT for 30 min and permeabilized with 0.5% Triton X-100 for 20 min. The cells were blocked using 2% bovine serum albumin in PBS at RT for 30 min, and then were incubated with primary anti-FLAG mouse mAb or anti-MYC mouse mAb (1:200) and primary anti-HA rabbit pAb (1:200) overnight at 4 $^{\circ}$ C. Next, cells were washed 3 \times in PBST (1–2 min per wash) and incubated with secondary antibodies Goat Anti-Mouse IgG H&L Alexa Fluor 594 (1:500) and Goat anti-Rabbit IgG H&L Alexa Fluor 647 (1:500). The cell nuclei were counter stained with 0.5 μ g/mL 4',6'-diamidino-2-phenylindole (DAPI, Beyotime, China) at 37 $^{\circ}$ C for 15 min. Finally, the coverslip with stained cells was loaded on slide, sealed by nail polish, and visualized by laser-scanning confocal microscope (LSCM, Leica SP8, Solms, Germany) at the excitation wavelengths 405 nm, 488 nm, 561 nm and 633 nm, respectively.

ASFV infection and S273R siRNA treatment

Primary PAMs were isolated from the lung lavage fluid of 4-week-old healthy piglets and maintained in RPMI-1640 medium containing 10% FBS. The ASFV genotype II positive samples from diseased pigs were inoculated into primary PAMs for virus culture and appearance of CPEs, and the fifth passaged ASFV was used for subsequent siRNA knockdown experiments. The primary PAMs (1×10^6 cells/well) were transfected with S273R siRNA and control siRNA (100 nM each, GenePharma) using Lipofectamine 2000, and 24 h later the transfected cells were infected with 0.01 MOI ASFV for another 72

h. The cells were harvested for RT-qPCR and Western blot analysis, respectively. All ASFV infection experiments were performed in the animal biosafety level 3 (ABSL-3) of Yangzhou University approved by the Ministry of Agriculture and Rural Affairs (-07140020201109-1). The animal experiment was in strict accordance with the Guidance for the Care and Use of Laboratory Animals of Yangzhou University (SYXK(JS)-2021-0026).

Statistical analysis

The data were the representative of three similar experiments and shown as the mean \pm SD. The statistical significance was determined by analysis with the software GraphPad Prism 8.0, where $p < 0.05$ was considered statistically significant as determined by the paired two-tailed t -test analysis. In the figures, “*”, “**” and “ns” denote $p < 0.05$, $p < 0.01$ and statistically not significant, respectively.

Results

The ASFV pS273R protein significantly inhibits cGAS-STING signaling activity

The cGAS serves as an essential cytosolic DNA sensor that upon activation quickly triggers STING-dependent signaling and results in transcriptions of type I interferon (IFN) genes and proinflammatory cytokine genes [16]. ASFV is a cytoplasmic dsDNA virus and mainly activates DNA-sensing cGAS-STING signaling pathway [17]. Recently, two studies reported that ASFV pDP96R and pA528R (MGF505-7R) suppress cGAS-STING pathway mediated production of IFNs and proinflammatory cytokines by targeting TBK1/IKK β and STING, respectively [18,19]. However, the question whether the cGAS-STING pathway is suppressed by other ASFV viral proteins still persists. In our study, we utilized the porcine cGAS-STING activated ISRE promoter assay and screened the ASFV genomic ORFs for modulators of cGAS-STING pathway (Supplementary Figure S1). The results showed that a number of ASFV genes exhibited an obvious inhibiting effect and were likely to play a role of immune evasion in the cGAS-STING pathway. These genes include MGF110-1L, MGF110-2L, MGF110-3L, MGF110-4L, MGF110-5-6L, MGF360-4L, X69R, MGF300-1L, MGF300-4L, MGF505-1R, MGF360-12L, MGF505-6R, MGF505-7R, A104R, A118R, A151R, F334L, F778R, EP152R, EP153R, EP402R, CP204L, CP80R, D345L, S183L, S273R, E120R, I215L and DP96R. Among these inhibitory genes, S273R encoding

pS273R was the most effective and showed reproducible suppression of cGAS-STING signaling which was not reported previously. Therefore, we pursued to investigate the inhibitory role of S273R in the cGAS-STING pathway.

We first confirmed the inhibitory role of pS273R using different promoter assays in transfected 293T cells, and found that co-transfection of pS273R in 293T cells could significantly inhibit ISRE, IFN β and NF- κ B promoter activity induced by porcine cGAS-STING signaling (Figure 1(a)). Co-transfection of porcine cGAS and STING activated downstream IFN β , ISG56, ISG60 and IL-8 gene transcriptions and the inductions of these gene transcriptions were significantly suppressed by the co-transfected pS273R (Figure 1(b)). Co-expression of porcine cGAS and STING led to the phosphorylation of TBK1 and IRF3, and downstream ISG56 production. The presence of pS273R restrained the phosphorylation of IRF3 and the production of ISG56, but retained the phosphorylation of TBK1 (Figure 1(c)).

In order to explore the effect of pS273R on endogenous porcine cGAS-STING signaling pathway, we used the PAMs stimulated by three different agonists, polydA:dT and 45bp dsDNA to activate cGAS, and 2'3'-cGAMP to activate STING. In promoter assays, we found that pS273R significantly inhibited polydA:dT and 2'3'-cGAMP activated ISRE and NF- κ B promoter activity (Figure 2(a)). In RT-qPCR assay, the downstream gene transcriptions of porcine IFN β , ISG56, IL-8 mRNA levels induced by polydA:dT (Figure 2(b)), 45bp dsDNA (Figure 2(c)) and 2'3'-cGAMP (Figure 2(d)) were all significantly inhibited by pS273R. Consistently, we also found that phosphorylation of IRF3 and expression of ISG56 were markedly decreased in PAMs in the presence of pS273R after polydA:dT stimulation (Figure 2(e)) and 2'3'-cGAMP stimulation (Figure 2(f)). However, in both cases, the phosphorylation of TBK1 was not affected by pS273R (Figure 2(e,f)). These results were perfectly in line with those from exogenous porcine cGAS-STING signaling pathway in transfected 293T cells (Figure 1).

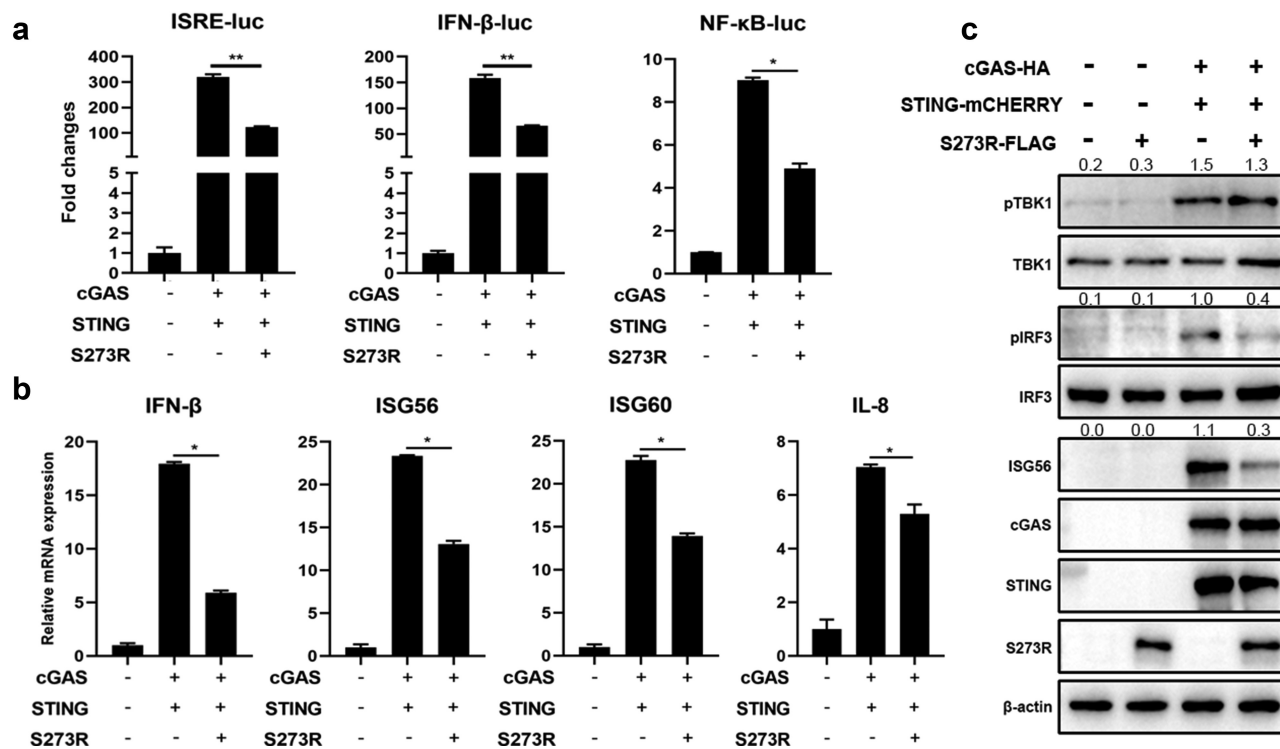


Figure 1. The effect of ASFV pS273R on the signaling activity of exogenous porcine cGAS-STING pathway. (a) HEK293T cells in 96-well plates (2×10^4 cells/well) were co-transfected with 20 ng cGAS-HA and 10 ng STING-mCHERRY, plus 10 ng ISRE-luc or IFN β -luc or NF- κ B-luc and 0.2 ng pRL-TK plasmid, along with 10 ng 3 \times FLAG-pCMV-S273R or control vector, which were normalized to 50 ng/well by control vector. At 24 h post-transfection, luciferase activities were detected using Double-Luciferase Reporter Assay. (b,c) HEK293T cells in 24-well plates (3×10^5 cells/well) were co-transfected with 400 ng cGAS-HA and 400 ng STING-mCHERRY plasmids together with 400 ng 3 \times FLAG-pCMV-S273R or control vector for 24 h, then the cells were harvested and analyzed by RT-qPCR for downstream gene expressions (b) and Western blotting using the indicated antibodies (c). The densitometry values of p-TBK1, p-IRF3 and ISG56 proteins after normalization were shown on top of the corresponding bands.

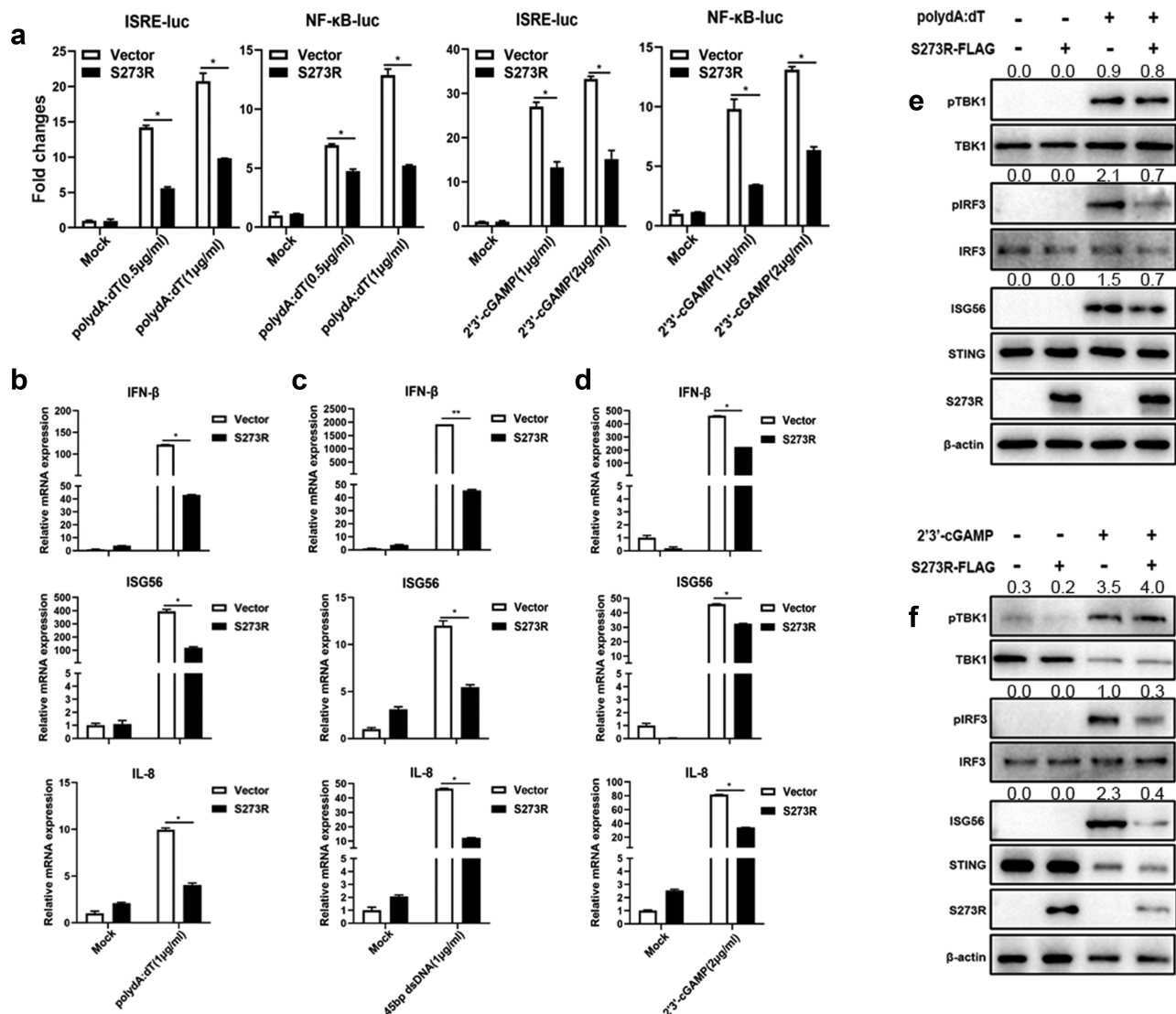


Figure 2. The effect of ASFV pS273R on endogenous porcine cGAS-STING signaling pathway. (a) PAMs in 96-well plates (2×10^4 cells/well) were co-transfected with 10 ng ISRE-luc or NF-κB-luc and 0.2 ng pRL-TK plasmids along with 20 ng 3×FLAG-pCMV-S273R or control vector, which were normalized to 50 ng/well by control vector. After 24 h, the cells were not or transfected with polydA:dt (0.5 μg/mL, 1 μg/mL) or 2'3'-cGAMP (1 μg/mL, 2 μg/mL) for 8 h. The luciferase activities were detected using Double-Luciferase Reporter Assay. (b–d) PAMs in 24-well plates (3×10^5 cells/well) were co-transfected with 1 μg 3×FLAG-pCMV-S273R or control vector for 24 h and then transfected with polydA:dt (1 μg/mL) (b) or 45bp dsDNA (1 μg/mL) (c) or 2'3'-cGAMP (2 μg/mL) (d) for 8 h. The harvested cells were measured by RT-qPCR for downstream gene expressions as indicated. (e–f) PAMs in 24-well plate (3×10^5 cells/well) were co-transfected with 1 μg 3×FLAG-pCMV-S273R or control vector for 24 h and then transfected with polydA:dt (1 μg/mL) or 2'3'-cGAMP (5 μg/mL) for 8 h. The harvested cells were detected by Western blotting with the indicated antibodies. The densitometry values of p-TBK1, p-IRF3 and ISG56 proteins after normalization were shown on top of the corresponding bands.

In addition, we also checked the effect of pS273R on the IRF3 and NF-κB p65 nuclear translocations. The results showed that in the presence of pS273R, 2'3'-cGAMP induced nuclear translocations of both IRF3 (Figure 3(a)) and p65 (Figure 3(b)) were inhibited. These results further consolidated the inhibitory function of pS273R. Taken together, our results clearly suggested that pS273R inhibits porcine DNA sensing cGAS-STING pathway.

ASFV pS273R disturbs the porcine cGAS-STING signaling pathway mediated antiviral function

The innate immune cGAS-STING signaling pathway is capable of sensing virus attack and induces an antiviral response [20]. To determine whether pS273R could disturb cGAS-STING mediated antiviral function, we selected two GFP viruses Herpes Simplex Virus-1

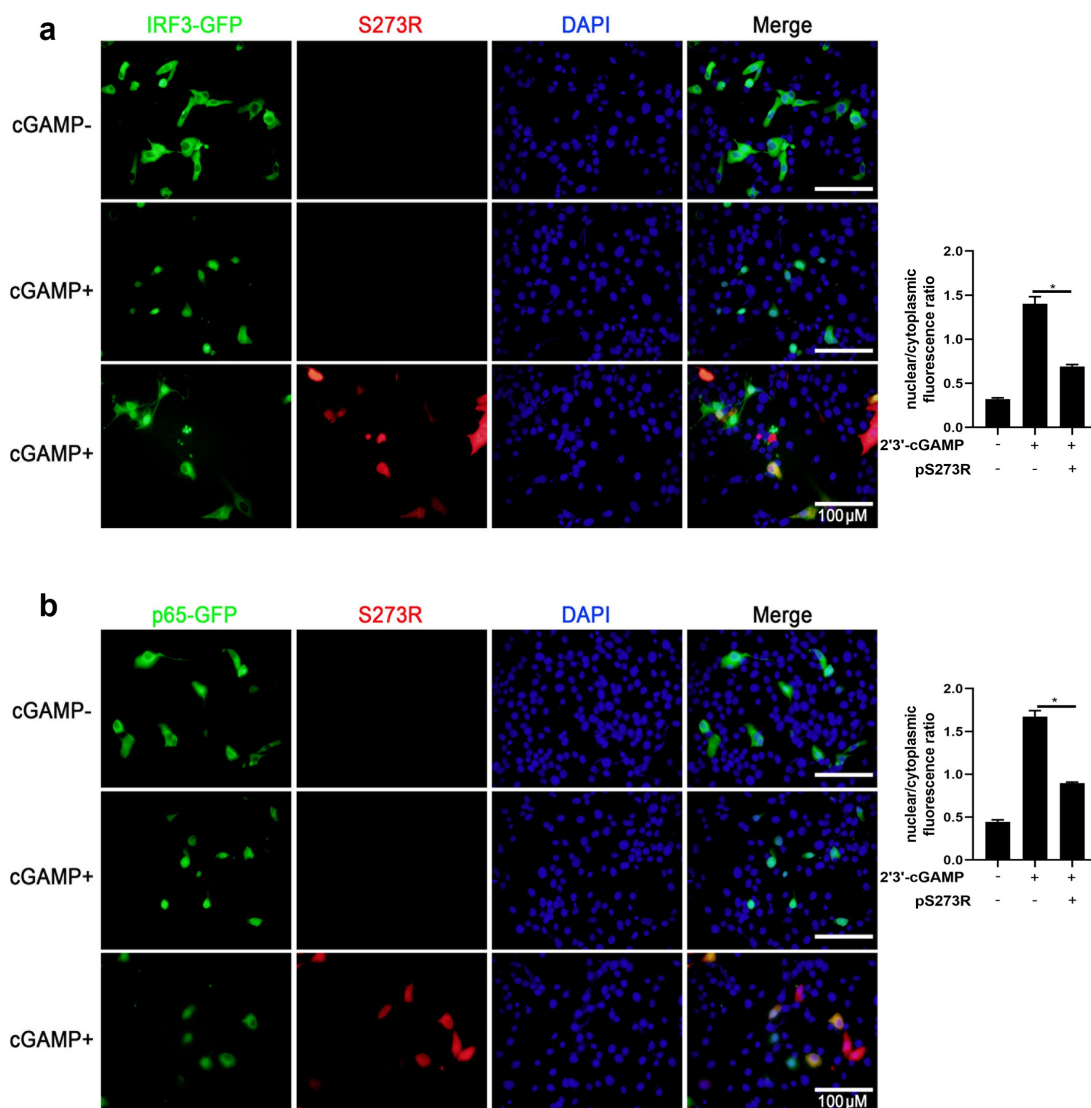


Figure 3. The effect of ASFV pS273R on nuclear translocations of IRF3 and NF- κ B p65. The PAMs grown on the coverslips in 24-well plates (1×10^5 cells/well) were transfected with (a) IRF3-GFP (0.5 μ g) and pCAGGS-S273R-2 HA (0.5 μ g) or control vector (0.5 μ g), (b) p65-GFP (0.5 μ g) and pCAGGS-S273R-2 HA (0.5 μ g) or control vector (0.5 μ g) using Lipofectamine 2000. at 18 h post translation, the cells were stimulated with transfection of 2'3'-cGAMP (1 μ g/ml) for another 6 h. the cells on coverslips were sequentially probed with rabbit anti-HA mAb, goat anti-rabbit IgG H&L Alexa Fluor 594, counter-stained with nucleus marker DAPI. the stained cells on coverslips were visualized by fluorescence microscope. the statistical analysis of the ratios of IRF3-GFP and p65-GFP in nuclear fractions vs cytoplasmic fractions were each shown on the right.

(HSV-1, a DNA virus) and Vesicular Stomatitis Virus (VSV, an RNA virus) to infect PAMs transfected with ASFV pS273R (Figures 4 and 5). The virus replications were examined by fluorescence microscopy, Western blotting, flow cytometry, RT-qPCR and TCID50 assay, respectively (Figures 4 and 5). We found that HSV-1 replicative GFP signals using MOI 0.01 and 0.1 were both enhanced in the presence of pS273R relative to controls under fluorescence microscopy (Figure 4(a)), by Western blotting (Figure 4(b)) and by flow cytometry analysis (Figure 4(c)). Using RT-qPCR, the HSV1 gB gene transcriptions were also upregulated with

pS273R, in sharp contrast with the downregulated IFN β and ISG56 genes (Figure 4(d)). Accordingly, the virus titers in the supernatants of PAMs infected with HSV1 of MOIs 0.01 and 0.1 were both increased relative to the controls in the TCID50 assay (Figure 4(e)).

The cGAS-STING pathway mediates a broad range of antiviral function including anti-DNA virus and anti-RNA virus activity, thus we also tested the role of pS273R during VSV replication (Figure 5). Similarly, the VSV replicative GFP signals using MOIs 0.001 and 0.01 were both enhanced relative to the controls under fluorescence microscopy (Figure 5(a)) and by flow

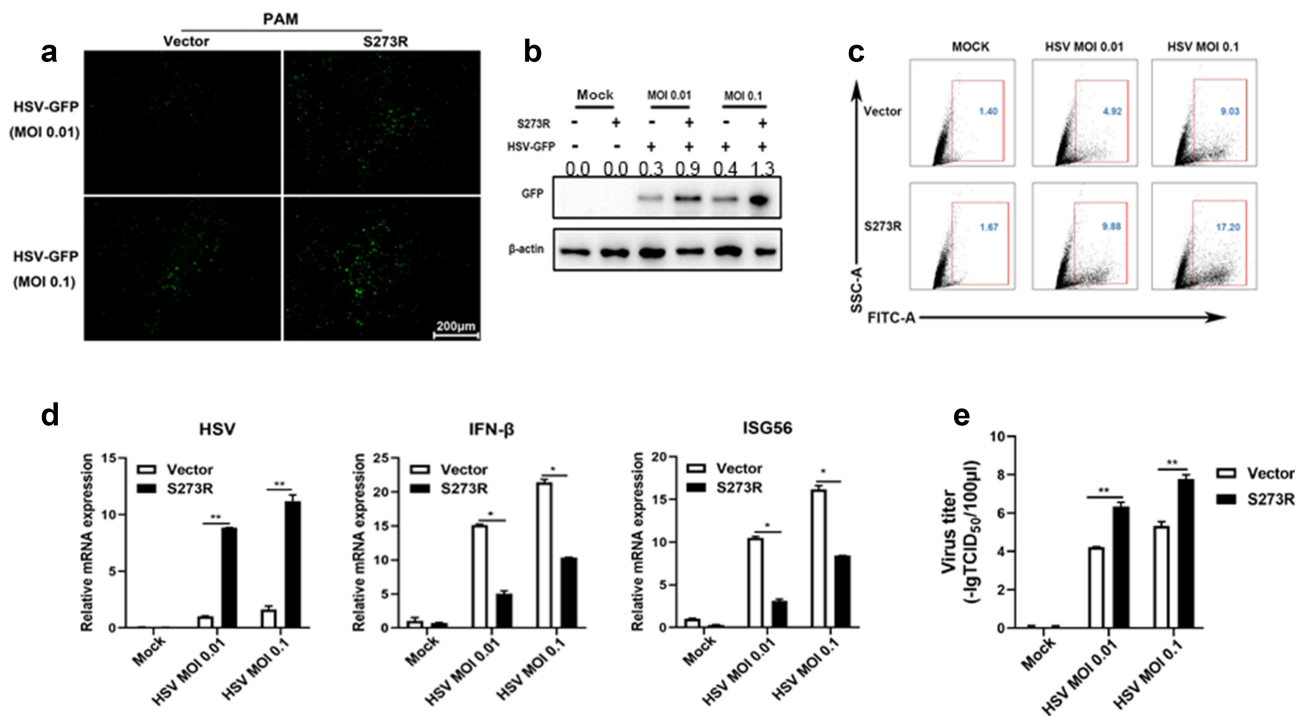


Figure 4. ASfV pS273R interfered the cGAS-STING signaling mediated anti-HSV-1 activity. (a,b) PAMs in 24-well plates (3×10^5 cells/well) were co-transfected with $1 \mu\text{g}$ 3×FLAG-pCMV-S273R or control vector for 24 h and then infected with .01 MOI or .1 MOI HSV-1-GFP for 36 h, the GFP signals were observed by fluorescence microscopy (a). The infected cells were harvested to measure the GFP protein expressions by Western blotting with the normalized densitometry values of GFP proteins shown on top of the corresponding bands. (b). (c) PAM cells in 6-well plates (8×10^5 cells/well) were co-transfected with $2 \mu\text{g}$ 3×FLAG-pCMV-S273R or control vector for 24 h and then infected with .01 MOI or .1 MOI HSV-1-GFP for 36 h, the GFP cells in infected PAMs were analyzed by flow cytometry. (D) The infected cells were harvested to measure HSV-1 gB gene and cellular gene transcriptions by RT-qPCR. (E) The viral titer in the supernatant from HSV-1 infected PAMs was measured by TCID50 assay.

cytometry (Figure 5(b)). In RT-qPCR, the VSV glycoprotein gene transcriptions were upregulated with pS273R (Figure 5(c)) in sharp contrast with the downregulated IFN β and ISG56 gene transcriptions (Figure 2 (e,f)). Accordingly, the virus titers in the supernatants of infected PAMs with VSV of MOIs 0.001 and 0.01 were both increased with the S273R compared with the controls by the TCID50 assay (Figure 5(d)) as well as by the plaque assay (Figure 5(g)). Collectively, these results demonstrated that pS273R could enhance virus replications by damaging cGAS-STING mediated antiviral functions.

ASfV pS273R negatively regulates the cGAS-STING signaling pathway by targeting IKK ϵ

To investigate the mechanism of how pS273R suppresses the cGAS-STING signaling pathway, pS273R was first co-transfected with individual signaling molecules of cGAS-STING-IFN pathway including TBK1 (Figure 6(a)), IKK ϵ (Figure 6(b)) or IRF3-5D (Figure 6(c)) into 293T cells and the downstream

ISRE, IFN β and NF- κ B promoter activity were examined. The results showed that only IKK ϵ but not TBK1 and IRF3-5D activated promoter activity were inhibited by pS273R (Figure 6(a-c)). The cGAS-STING signaling also activates downstream NF- κ B and pro-inflammatory cytokines even though the strength is much weaker and the associated molecular details are not clear. Thus, the signaling activity of NF- κ B relevant molecules IKK β and p65 were also checked in the presence of pS273R by NF- κ B promoter assay, and it turned out that no inhibitory effect of pS273R was observed (Figure 6(d,e)). Since only IKK ϵ was affected by pS273R, the IKK ϵ induced downstream gene transcriptions were examined by RT-qPCR, and the results showed that the IKK ϵ induced downstream IFN β , ISG56 and IL-8 gene levels were inhibited by pS273R in dose-dependent manners (Figure 6(f)), which is consistent with the promoter assays (Figure 6(b)).

Next, the IKK ϵ -induced signaling was examined by Western blotting (Figure 6(g)). Ectopic IKK ϵ was able to activate the phosphorylations of TBK1 and IRF3 and the downstream ISG56 production as previously reported

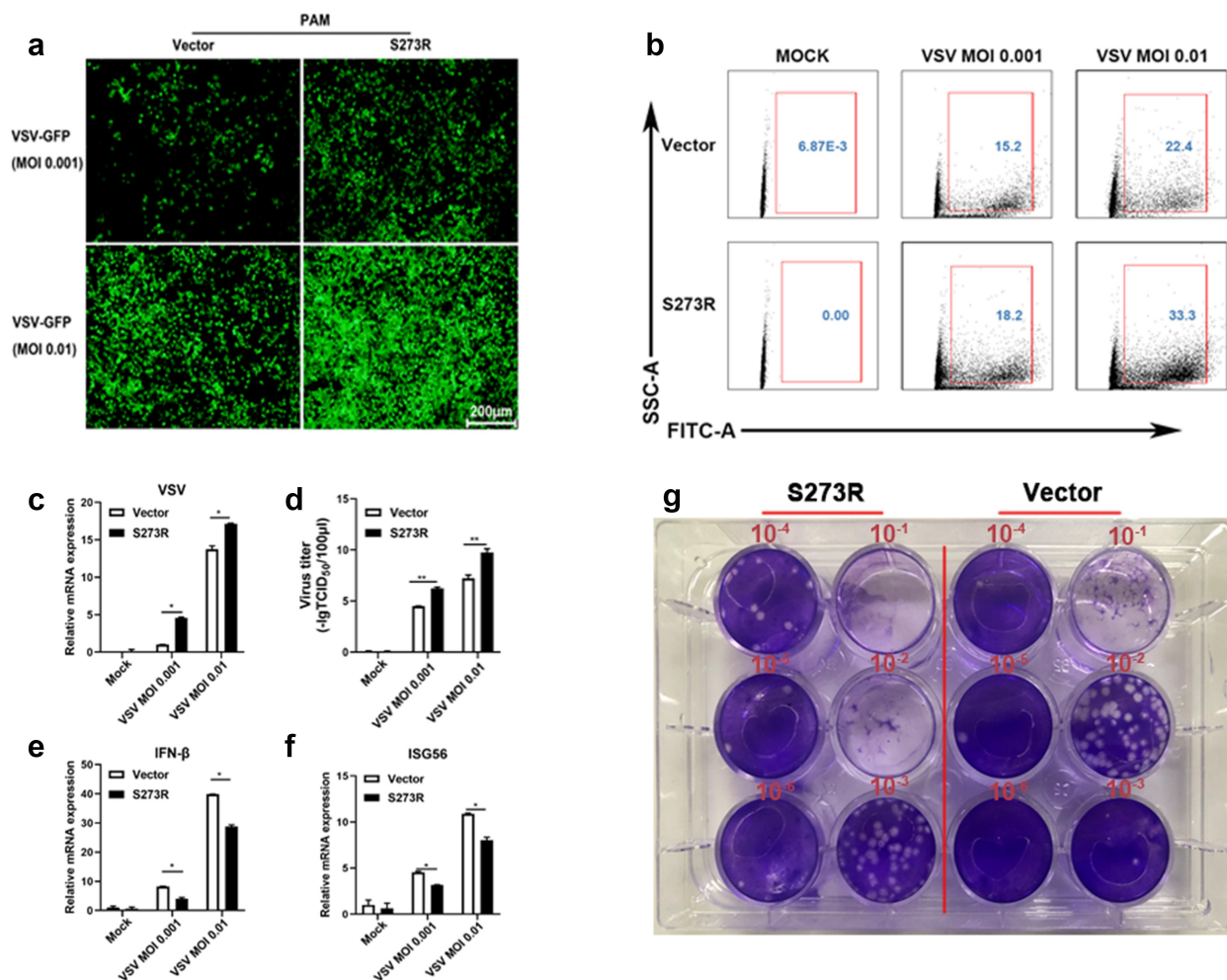


Figure 5. pS273R inhibited cGAS-STING signaling mediated anti-VSV function. (a) PAMs in 24-well plates (3×10^5 cells/well) were co-transfected with $1 \mu\text{g}$ 3 \times FLAG-pCMV-S273R or empty vector for 24 h and then infected with .001 MOI or .01 MOI VSV for 16 h. The GFP signals were observed by fluorescence microscopy. (b) PAM cells in 6-well plates (8×10^5 cells/well) were co-transfected with $2 \mu\text{g}$ 3 \times FLAG-pCMV-S273R or control vector for 24 h and then infected with .001 MOI or .01 MOI VSV for 16 h, the GFP cells in infected PAMs were analyzed by flow cytometry. (c–g) the infected cells were harvested to measure VSV glycoprotein gene (c) and cellular gene transcriptions (e, f) by RT-qPCR. The viral titer in the supernatant from VSV infected PAMs was measured by TCID₅₀ assay (d) and plaque assay (g).

[21]. In the presence of pS273R, the IRF3 phosphorylation and ISG56 induction were inhibited, but once again TBK1 phosphorylation was not affected (Figure 6(g)). Finally, the IKK ϵ induced antiviral activity was also investigated in the presence of pS273R (Figure 6(h–j)). IKK ϵ exhibited obvious anti-HSV1 activity, however, in the presence of pS273R, the IKK ϵ mediated anti-HSV1 activity was weakened as observed by fluorescence microscopy (Figure 6(h)), shown by RT-qPCR (Figure 6(l)) and TCID₅₀ assay (Figure 6(j)). Similarly, pS273R promoted the VSV replications by damaging IKK ϵ mediated antiviral function (Sup Figure S2). Collectively, these results illustrated that pS273R inhibited cGAS-STING signaling pathway by targeting IKK ϵ .

ASFV pS273R interacts with IKK ϵ and disturbs the interaction between IKK ϵ and STING

IKK ϵ is a crucial IKK-related kinase that is significant for innate immune signaling, yet the interaction of STING and IKK ϵ is still not clear. We first assessed the interaction between IKK ϵ and STING by Co-IP, and the result showed that there was an obvious interaction between IKK ϵ and STING (Figure 7(a)). Since pS273R targets IKK ϵ and inhibits its activity, the interaction between pS273R and IKK ϵ was also discernible in Co-IP assay (Figure 7(c)). However, there was no interaction between pS273R and STING in Co-IP assay (Figure 7(b)). Consistent results were shown for cellular co-localization between these proteins in PAMs by con-

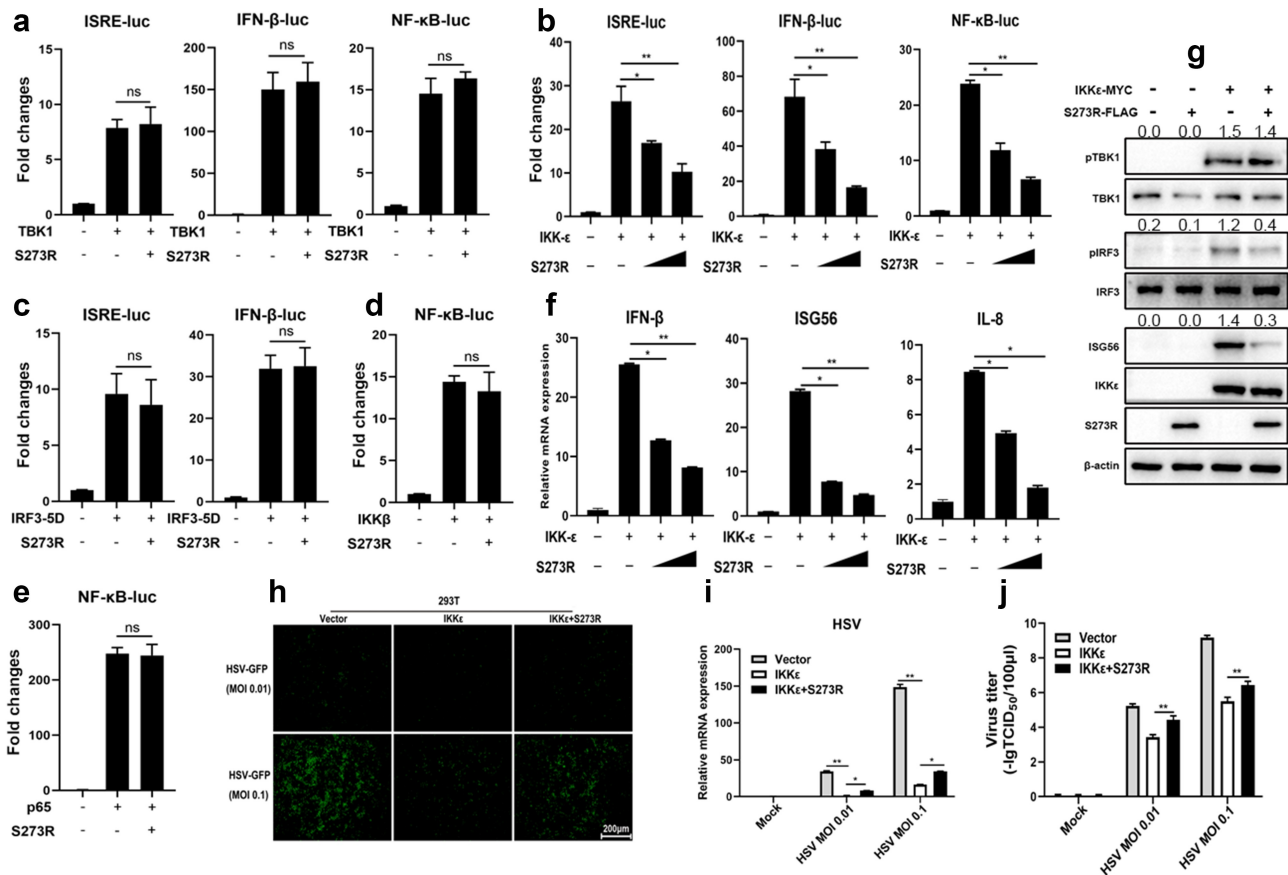


Figure 6. The identification of IKK ϵ as the cellular target by ASFV pS273R. (a–e) HEK293T cells were co-transfected with 20 ng TBK1 expression plasmids and 10 ng 3 \times FLAG-pCMV-S273R (a), with 20 ng IKK ϵ expression plasmid and increased amounts of pS273R (10 ng or 20 ng) (b), with 20 ng IRF3-5D expression plasmid and 10 ng pS273R (b), with 20 ng IKK β plasmid and 10 ng pS273R (d), with 20ng p65 plasmid and 10 ng pS273R (e), plus 10 ng ISRE-luc, IFN β -luc or NF- κ B-luc and 0.2 ng pRL-TK plasmids, which were normalized to 50 ng/well by vector 3 \times FLAG-pCMV. After 24 h, the luciferase activities were detected using Double-Luciferase Reporter Assay. (f,g) pS273R plasmid (400 ng or 800 ng) were co-transfected with 400 ng IKK ϵ into HEK293T cells. After 24 h, the cells were harvested and analyzed by RT-qPCR (f) and Western blotting (g). (h–j) the IKK ϵ plasmid (500 ng) were co-transfected with 500 ng pS273R plasmid or empty vector into 293T cells for 24 h, then the transfected 293T cells were infected with 0.01 MOI or .1 MOI HSV-1-GFP for 36 h, the GFP signals were observed by fluorescence microscopy (H). the infected cells were harvested to measure the HSV-1 gene expression by RT-qPCR (i). the viral titer in the supernatant from HSV-1 infected 293T cells was measured by TCID₅₀ assay (j).

focal microscopy (Figure 7(e)). Obvious co-localization between IKK ϵ and STING, co-localization between IKK ϵ and pS273R, and no co-localization between pS273R and STING were observed (Figure 7(e)). The co-localization of STING and IKK ϵ was so obvious that the formation of puncta was appreciated (Figure 7(e)). However, in the Co-IP assay and in the presence of pS273R, the interaction between IKK ϵ and STING was disturbed in a pS273R dose-dependent manner (Figure 7(d)). These results indicated that ASFV pS273R blocks the interaction between STING and IKK ϵ in a dose-dependent manner to evade host innate immunity.

The protease activity of pS273R is responsible for inhibition of porcine cGAS-STING signaling pathway

A recent study about the structural information of pS273R revealed that a catalytic triad of C232-H168-N187 and the regions spanning amino acids 1–20 and 256–273 of pS273R play essential roles in pS273R enzyme activity [22]. To explore the potential roles of these active sites of pS273R in the inhibitory function, we generated three-point mutants (H168R, N187A and C232S) and two truncated mutants (Δ N1–20 and

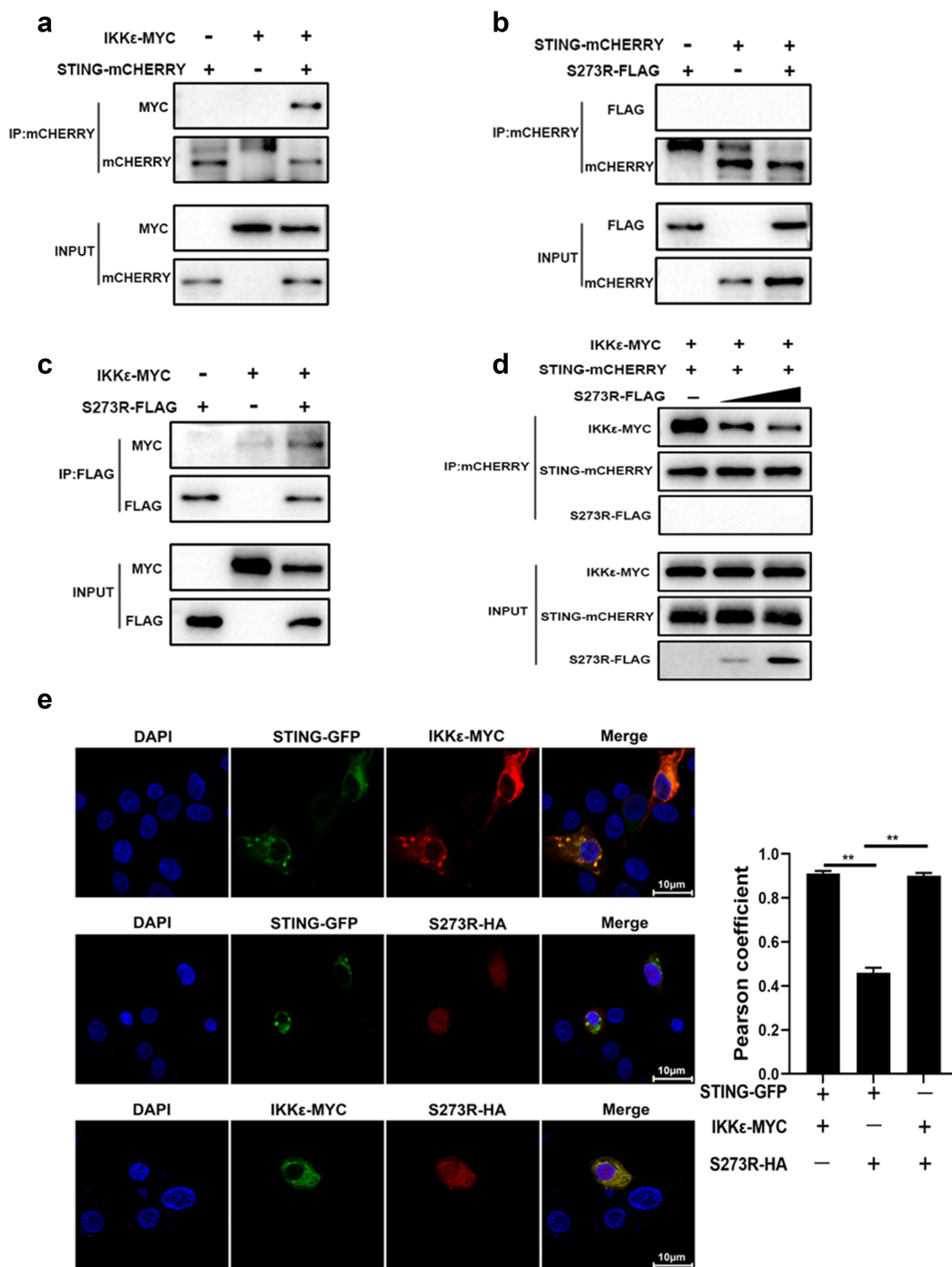


Figure 7. pS273R interacted with IKKε and disturbed the interaction between IKKε and STING. (a–c) HEK293T cells in 6-well plates (8×10^5 cells/well) were co-transfected with 1 μ g each plasmid as indicated for 48 h and then the cells were harvested and subjected for Co-IP using the indicated antibodies and subsequent Western blot analysis. (d) Increasing amounts of pS273R plasmid (1 μ g, 2 μ g) were co-transfected with 1 μ g STING-mCHERRY and 1 μ g IKKε-MYC into 293T cells for 48 h and then cells were harvested and immunoprecipitated with anti-mCHERRY antibody and subjected to Western blot analysis. (E) PAM cells in 24-well plates (3×10^5 cells/well) were co-transfected with STING-GFP (0.5 μ g) and IKKε-MYC (0.5 μ g), with STING-GFP (0.5 μ g) and pS273R-HA (0.5 μ g), with IKKε-MYC (0.5 μ g) and pS273R-HA (0.5 μ g) for 24 h, and then cells were fixed and examined for cellular co-localization by confocal microscopy. The co-localizations in multiple vision fields were analyzed using Image J, and the Pearson coefficient values from 10 positive cells were graphed and shown on the right. The value of Pearson coefficient reflects the level of co-localization, with 1 representing 100% co-localization.

Δ N256–273) (Figure 8(a)). These enzyme inactive mutants were tested for inhibition of cGAS-STING signaling in various promoter assays. As shown in Figure 8(b), the inhibitory effects of the five mutants disappeared to varying degrees. Furthermore, the inhibitory effects of the five mutants on IKK ϵ activated promoter activity also disappeared (Figure 8(c)). To figure out whether these five mutants could disturb STING interaction with IKK ϵ , the Co-IP of STING and IKK ϵ was performed in the presence of each pS273R mutants, and the results showed that the pS273R mutants lost the ability to disturb the interaction of STING and IKK ϵ (Figure 8(d)), except the mutant H168R that is close to wild-type pS273R, also reflected by the remained inhibition of cGAS-STING mediated ISRE and IFN β promoter activity (left and middle, Figure 8(b)). The cellular co-localizations between STING and IKK ϵ in the presence of pS273R mutants were examined and the results showed that with the pS273R, the co-localized puncta of STING and IKK ϵ disappeared, whereas in the presence of mutants except H168R, the significant co-localized puncta were maintained (Sup Figure S3). The mutant

H168R exhibited kind of difference from other mutants although the reason is not known.

The pS273R mediated IKK ϵ de-sumoylation likely contributes to inhibition of porcine cGAS-STING signaling pathway and replication of ASFV

It appeared that pS273R protease activity plays a critical role in the inhibition of cGAS-STING signaling as well as inhibition of IKK ϵ activity. However, we did not observe the cleavage of IKK ϵ and related signaling proteins, we wondered if pS273R, as a SUMO-1 protease, might affect the sumoylation modification of the target protein and its subsequent function. To test this hypothesis, we detected the IKK ϵ status in the presence of sumo proteins and found that IKK ϵ was sumoylated in the presence of sumo-3 (Figure 9(a)). Whereas pS273R was able to suppress the IKK ϵ sumoylation (Figure 9(a)), as well as cell sumo-2/3 (Figure 9(b)). Secondly, we chose 2-D08, a unique inhibitor of SUMOylation [23,24], to evaluate the hypothesis. 2-D08 was confirmed to be inhibitory to the cell sumo-2/3 (Figure 9(c)). The results showed that 2-D08 could markedly inhibit the IFN β , ISG56 and

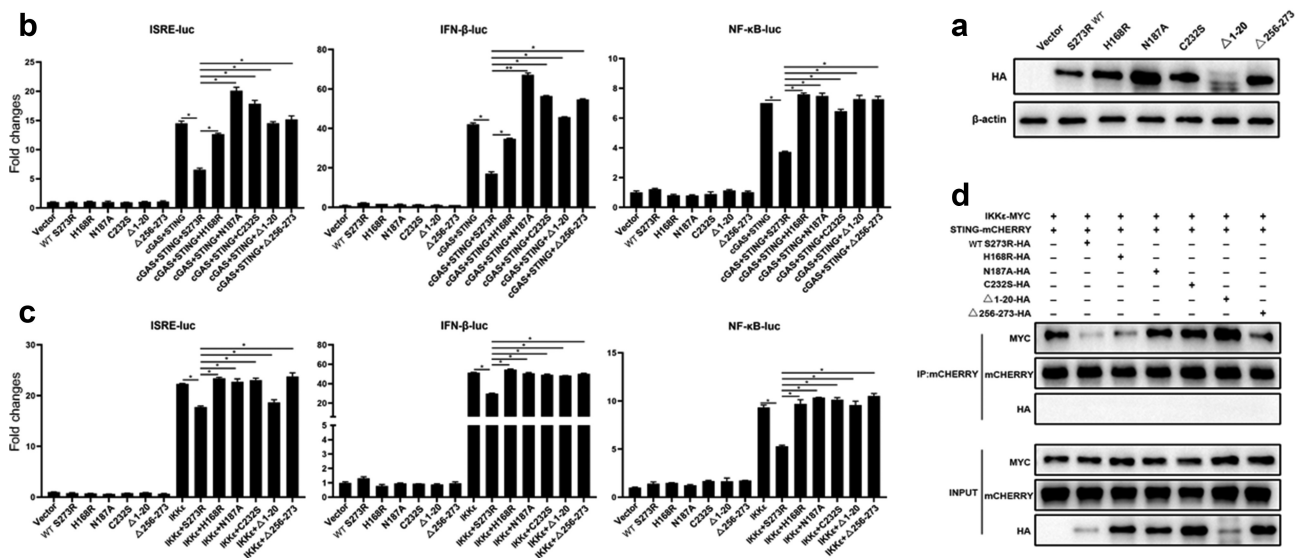


Figure 8. pS273R mutants without protease activity had decreased suppression on IKK ϵ of cGAS-STING pathway. (a) HEK293T cells were co-transfected with 1 μ g of each pS273R mutants plus wild type (WT), respectively, and then the cells were harvested and analyzed by Western blotting. (b) HEK293T cells in 96-well plates (2×10^4 cells/well) were co-transfected with 20 ng cGAS-HA and 10 ng STING-mCHERRY, plus 10 ng ISRE-luc or IFN β -luc or NF- κ B-luc and 0.2 ng pRL-TK plasmid, along with 10 ng pS273R WT or pS273R mutants, which were normalized to 50 ng/well by vector pCAGGS. At 24 h post-transfection, luciferase activities were detected using Double-Luciferase Reporter Assay. (c) HEK293T cells were co-transfected with 20 ng IKK ϵ , plus 10 ng ISRE-luc or IFN β -luc or NF- κ B-luc and 0.2 ng pRL-TK plasmid, along with 10 ng pS273R WT or pS273R mutants, which were normalized to 50 ng/well by vector pCAGGS. After 24 h, luciferase activities were measured. (d) Each pS273R mutants (1 μ g) and WT were co-transfected with STING-mCHERRY (1 μ g) and IKK ϵ -MYC (1 μ g) into 293T cells for 48 h, and then the cells were harvested and subjected for Co-IP using anti-mCHERRY antibody and subsequent Western blot analysis.

IL-8 mRNA induction levels in dose manners upon either polydA:dT stimulation or 2'3'-cGAMP stimulation (Sup Figure S4(a,b)). The inhibitor 2-D08 also

inhibited cGAS-STING signaling induced IFN β and ISG56 mRNA levels in transfected 293T cells (Sup Figure S4(c)). Analogously, 2-D08 was able to inhibit

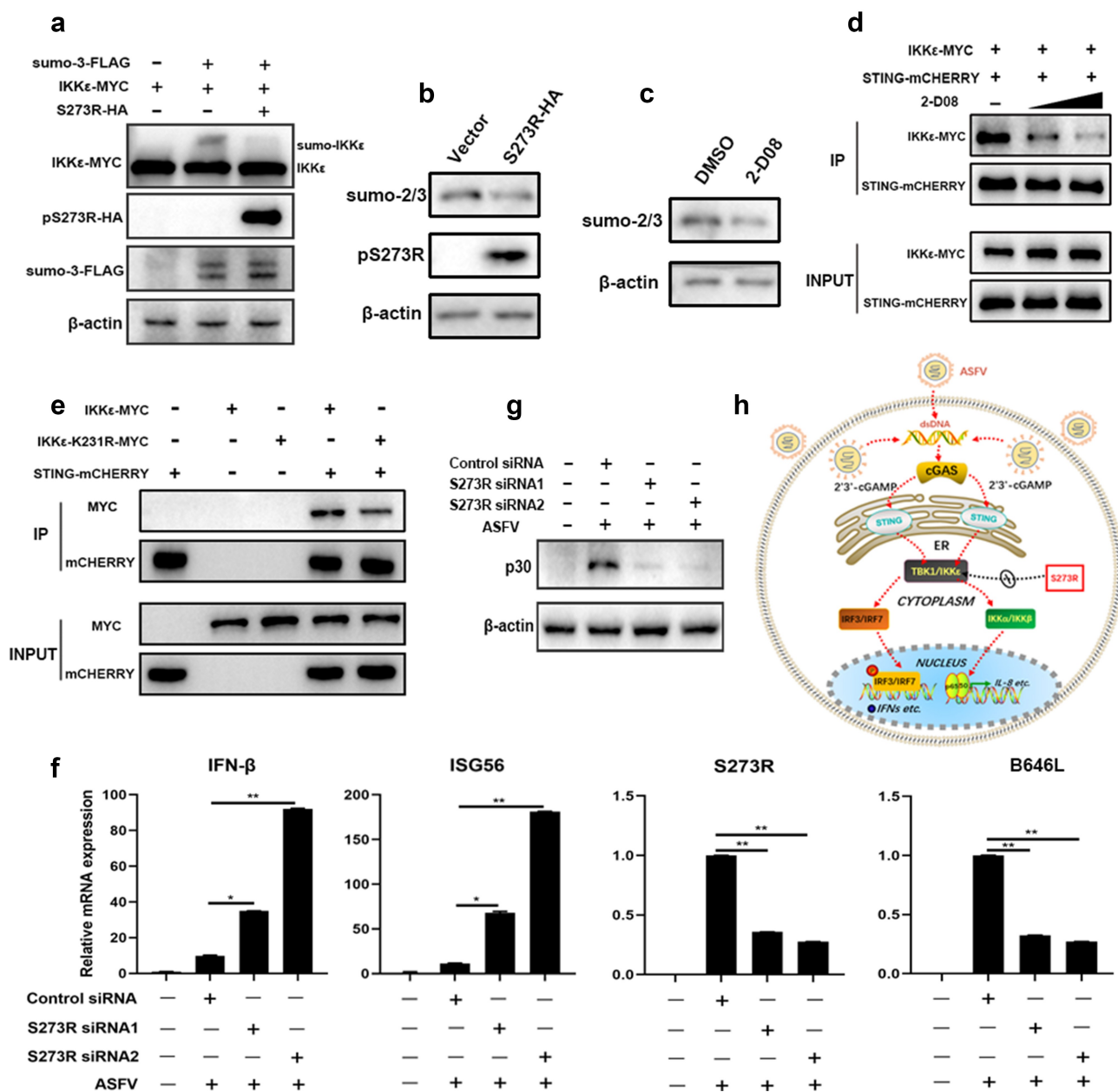


Figure 9. The inhibitory effect of pS273R on IKK ϵ sumoylation and the role of pS273R in ASFV caused IFN evasion. (a) HEK293T cells in 24-well plates (3×10^5 cells/well) were co-transfected with 300 ng IKK ϵ -MYC and 300 ng 3 \times FLAG-pCMV-sumo-3 plasmids together with 300 ng S273R-HA or control vector for 24 h, then the cells were harvested and analyzed by Western blotting using the indicated antibodies. (b) HEK293T cells in 6-well plates (8×10^5 cells/well) were transfected with 1 μ g pS273R plasmid or vector control for 24 h, and then the cells were harvested and subjected for Western blot analysis. (c) HEK293T cells in 24-well plate were treated with 2-D08 (50 μ M) or DMSO control for 18 h, followed by Western blotting with anti-sumo2/3 antibody. (d) HEK293T cells in 6-well plates (8×10^5 cells/well) were co-transfected with STING-mCHERRY (1 μ g) and IKK ϵ -MYC (1 μ g) for 24 h and then treated with 2-D08 (50 μ M, 100 μ M) for 18 h. the cells were harvested and subjected for Co-IP using anti-mCHERRY antibody and subsequent Western blot analysis. (e) IKK ϵ -MYC and K231R mutant (1 μ g each) plus STING-mCHERRY (1 μ g) were transfected into 293T cells for 48 h, and then the cells were subjected for Co-IP using anti-mCHERRY antibody and subsequent Western blot analysis. (f,g) Primary PAMs (1×10^6 cells/well) were transfected with siRNA for 24 h and then infected with 0.01 MOI ASFV for another 72 h. the cells were harvested for RT-qPCR analysis of the indicated gene transcriptions (f) and Western blot analysis of ASFV p30 protein (g). (h) the schematic diagram of ASFV pS273R antagonism on IKK ϵ of cGAS-STING signaling pathway.

the interaction of IKK ϵ and STING in Co-IP assay in a dose-dependent manner (Figure 9(d)). Additionally, K231 was reported as the only IKK ϵ sumoylation location and the sumoylation of IKK ϵ is the prerequisite for IKK ϵ function [25]. We made the IKK ϵ mutant K231R and tested its activity and the interaction with STING. The results showed that K231R mutant exhibited substantial reduction of ISRE and NF- κ B activities relative to wild-type IKK ϵ (Sup Figure S5(a)). Further, K231R had impaired interaction with STING in Co-IP assay (Figure 9(e)) and did not interact with pS273R any more (Sup Figure S5(b)).

To test the role of pS273R in the IFN induction in the context of ASFV infection, we treated the primary porcine alveolar macrophages with S273R siRNA before ASFV infection. The results showed that, relative to control siRNA, the ASFV-induced IFN β and ISG56 gene transcriptions were both upregulated with either of the two S273R siRNAs, accompanied by the decreased viral S273R and B646 L gene transcriptions and p30 protein expression (Figure 9(f,g)). Taken together, these data demonstrate that pS273R likely acts as an inhibitor of IKK ϵ sumoylation to obstruct the interaction of IKK ϵ and STING, suppress the cGAS-STING signaling and thus evade antiviral function.

Discussion

Many viruses are equipped to promote the replications and establish persistent infections in host. Therefore, viruses must evolved multiple mechanisms to antagonize the antiviral immune responses to achieve the immune evasion. Likewise, ASFV has developed multiple strategies to evade innate immune system, including modulation of type I IFN responses, inhibition of apoptosis, inhibition of autophagy and inhibition of inflammatory responses *etc*, with few of the corresponding viral proteins identified [26,27]. However, ASFV long double-stranded DNA genome codes for more than 150 proteins of which many are non-essential for viral replication in cells and their potential roles and the mechanism of action in evading the host's defenses are still unknown. Here, we revealed for the first time that pS273R plays as a negative regulator in the cGAS-STING pathway via genomic ORF screening and confirming experiments (Figures 1 and 3 and Sup Figure S1). We also found that pS273R obviously promotes the replications of both DNA and RNA viruses (Figures 4 and 5), suggesting that pS273R facilitates their replications by damaging the cGAS-STING signaling which has been shown to have broad antiviral function [28].

Surprisingly, our results showed that pS273R inhibits the cGAS-STING signaling pathway by targeting and impairing the function of IKK ϵ (Figure 6). In the context of virus infections, pS273R has been observed to disturb IKK ϵ mediated antiviral function (Figure 6 and Sup Figure S2). The above results suggested that IKK ϵ is likely to play an important role in the cGAS-STING pathway. Indeed, IKK ϵ interacts with STING and the interaction can be disturbed by pS273R that interacts with IKK ϵ but not with STING (Figure 7). Therefore, our findings support that pS273R certainly acts on IKK ϵ to impair the antiviral function and help virus evade host defense. IKK ϵ has been previously reported to recruit and phosphorylate IRF3/7 in RIG-I-like receptors (RLR) and Toll-like receptors (TLR) signaling pathways [29,30], whereas it has been long believed that TBK1 acts as the only downstream kinase to mediate the cGAS-STING pathway to activate IFN production. However, one recent study showed that IKK ϵ synergizes redundantly with TBK1 to mediated STING activated NF- κ B signaling and inflammatory cytokine production, and on the other hand, IKK ϵ also participates in STING activated IFN production even though to a much less degree [31]. The phosphorylation of porcine STING Ser365 (Ser366 in humans) is mediated by active TBK1, but the phosphorylation site of STING by IKK ϵ in the absence of TBK1 is still not clear [31]. Therefore, our findings indicate that IKK ϵ is actually significant for the activation of the STING-dependent DNA sensing pathway, though the mechanism was unclear, which is warranted for future investigation.

Many positive-strand RNA viruses and retroviruses encode polyproteins or polyprotein precursors that are cleaved by viral proteases to form vital components of the virus particle, which are critical for virus maturation and infectivity [32]. The ASFV pS273R protease, as a member of SUMO-1-specific protease family, could accurately cleave two polyproteins, pp220 and pp62, at Gly-Gly-Xaa sites to produce important proteins required for ASFV morphogenesis [10]. In this study, we found that the protease activity of pS273R is required for inhibition of the interaction of IKK ϵ and STING and subsequent signaling (Figure 8); therefore, it is possible that pS273R protease inhibits the interaction of STING and IKK ϵ by cleaving the IKK ϵ . However, neither IKK ϵ nor STING expression was changed in the presence of pS273R. The ASFV pS273R protease consists of arm domain and core domain. While the arm domain is unique, the core domain shares similar structure fold and active triad to those of other SUMO-1 cysteine proteases, which contain Ubl (ubiquitin-like protein)-specific proteases (Ulp) in yeast and sentrin-specific proteases (SENP) in

mammals [33,34]. These proteases mainly catalyze the deconjugation of SUMOylated proteins; and accordingly, it is well known that some viral proteases have the ability to deconjugate certain small protein modifications to interrupt host innate immune responses [7,35,36]. Therefore, it is also possible that pS273R protease could inhibit interaction of STING and IKKε by cleaving small protein modification such as sumoylation of IKKε. Indeed, the pS273R inhibits IKKε sumoylation and cell sumo-2/3 (Figure 9(a,b)). Sumoylation inhibitor 2-D08 suppresses the interaction of STING and IKKε, and the cGAS-STING signaling activity, certifying the function of pS273R protease in the cGAS-STING pathway (Figure 9(d) and Sup Figure S4). The mutation of sumoylation site of IKKε decreases its activity and interaction with STING (Figure 9(e) and Sup Figure S5).

The papain-like proteases from coronaviruses and arteriviruses are known to be anchored in double membrane vesicles, exerting deubiquitinating or deISGylating activity on the accessed cell proteins to suppress antiviral innate immunity [37,38]. Previous study showed that pS273R is incorporated in viral particles, localized at viral factory (VF) and weakly scattered throughout cytoplasm [9], which is different from pS273R cellular localization in transfected cells (Figures 3 and 7(e)) of this study. Nevertheless, at late stage of ASFV replication, the VF disrupts and reorganizes many cell organelles [39], and likely IKKε/STING complex is brought proximity to pS273R in VF or in the scattered viral particles in cytoplasm. Thus, our findings are able to match up to pS273R during ASFV infection and reflect the situations of papain-like proteases from coronavirus and arteriviruses. Our study presents clear and relevant evidence that pS273R protease acts as a sumoylation inhibitor and targets IKKε modification to interfere with the immune response. During revision of this paper, the work published by Zhao *et al.* showed the pS273R exerts its protease activity to non-canonically cleave gasdermin D, disturb inflammasome-induced cell pyroptosis and promote ASFV replication [40]. Collectively, all these work explored different aspects of immune evasion by pS273R and broaden our understanding of immune evasion mechanism by ASFV.

In summary, upon infection of ASFV, porcine cytosolic cGAS senses the dsDNA of virus and catalyzes the synthesis of the second messenger cyclic GMP-AMP 2'3'-cGAMP), which binds and activates the adaptor STING. The oligomerized STING transfers from the endoplasmic reticulum (ER) to the trans-Golgi apparatus network (TGN); during the process, the TBK1 and

IKKε as well are recruited, phosphorylated and activated. TBK1 and IKKε subsequently phosphorylate the IRF3/7 and activate IKKα/IKKβ, inducing expression of the interferons and inflammatory factors (Figure 9(h)). However, ASFV pS273R could antagonize the cGAS-STING signaling pathway by targeting the IKKε, thus achieving immune escape (Figure 9(h)).

Disclosure statement

No potential conflict of interest was reported by the author(s).

Funding

The work was partly supported by the National Key Research and Development Program of China [2021YFD1800100], Jiangsu provincial key R & D plan [BE2020398], Jiangsu agricultural science and technology independent innovation fund project [CX(21)2035], the National Natural Science Foundation of China [32172867; 31872450], and A Project Funded by the Priority Academic Program Development of Jiangsu Higher Education Institutions (PAPD). Dr. Qing Chen is supported by Beijing Natural Science Foundation [6202002].

Author contribution statement

J.Z conceived and designed the experiments; J.L, J.Z, J.N, S.J, N.X, Y.G, Q.S, Q.C (Qi Cao) performed the experiments; W. Z, N.C, Q.Z, H.C, H.Z, F.M, J.Z analyzed the data; Q.C (Qing Chen) provided resources; J.L and J.Z wrote the paper. All authors contributed to the article and approved the submitted version.

Data availability statement

Data available within the article or its supplementary materials.

ORCID

Jianzhong Zhu  <http://orcid.org/0000-0002-7082-1993>

References

- [1] Anderson EC, Hutchings G, Mukarati N, et al. African swine fever virus infection of the bushpig (*Potamochoerus porcus*) and its significance in the epidemiology of the disease. *Vet Microbiol.* 1998;62(1):1–15.
- [2] Bastos A, Penrith M, Macome F, et al. Co-Circulation of two genetically distinct viruses in an outbreak of African swine fever in Mozambique: no evidence for individual co-infection. *Vet Microbiol.* 2004;103(3–4):169–182.

- [3] Montgomery RE. On a form of swine fever occurring in British East Africa (Kenya Colony). *J Comp Pathol Therap.* 1921;34:159–191.
- [4] Kolbasov D, Titov I, Tsybanov S, et al. African swine fever virus, Siberia, Russia, 2017. *Emerg Infect Dis.* 2018;24:796–798.
- [5] Zhou X, Li N, Luo Y, et al. Emergence of African swine fever in China, 2018. *Transbound Emerg Dis.* 2018;65(6):1482–1484. DOI:10.1111/tbed.12989
- [6] Galindo I, Alonso C. African swine fever virus: a review. *Viruses.* 2017;9:103.
- [7] Alejo A, Matamoros T, Guerra M, et al. A proteomic atlas of the African swine fever virus particle. *J Virol.* 2018;92. DOI:10.1128/JVI.01293-18
- [8] Dixon L, Chapman D, Netherton C, et al. African swine fever virus replication and genomics. *Virus Res.* 2013;173(1):3–14.
- [9] Andres G, Alejo A, Simon-Mateo C, et al. African swine fever virus protease, a new viral member of the SUMO-1-specific protease family. *J Biol Chem.* 2001;276:780–787.
- [10] Alejo A, Andrés G, Salas M. African swine fever virus proteinase is essential for core maturation and infectivity. *J Virol.* 2003;77:5571–5577.
- [11] Kumar H, Kawai T, Akira S. Pathogen recognition by the innate immune system. *Int Rev Immunol.* 2011;30:16–34.
- [12] Chen Q, Sun L, Chen ZJ. Regulation and function of the cGAS–STING pathway of cytosolic DNA sensing. *Nat Immunol.* 2016;17:1142–1149.
- [13] Zhang X, Bai X-C, Chen ZJ. Structures and mechanisms in the cGAS-STING innate immunity pathway. *Immunity.* 2020;53:43–53.
- [14] Tanaka Y, Chen ZJ. STING specifies IRF3 phosphorylation by TBK1 in the cytosolic DNA signaling pathway. *Sci Signal.* 2012;5:ra20–ra. DOI:10.1126/scisignal.2002521
- [15] Zheng W, Zhou R, Li S, et al. Porcine IFI16 negatively regulates cGAS signaling through the restriction of DNA binding and stimulation. *Front Immunol.* 2020;11:1669.
- [16] Kato K, Ishii R, Goto E, et al. Structural and functional analyses of DNA-sensing and immune activation by human cGAS. *PLoS One.* 2013;8:e76983.
- [17] Garcia-Belmonte R, Perez-Nunez D, Pittau M, et al. African swine fever virus armenia/07 virulent strain controls interferon beta production through the cGAS-STING pathway. *J Virol.* 2019;93. DOI:10.1128/JVI.02298-18
- [18] Wang X, Wu J, Wu Y, et al. Inhibition of cGAS-STING-TBK1 signaling pathway by DP96R of ASFV China 2018/1. *Biochem Biophys Res Commun.* 2018;506:437–443.
- [19] Li D, Yang W, Li L, et al. African swine fever virus MGF-505-7R negatively regulates cGAS-STING-mediated signaling pathway. *J Immunol.* 2021;206:1844–1857.
- [20] Ma Z, Damania B. The cGAS-STING defense pathway and its counteraction by viruses. *Cell Host Microbe.* 2016;19:150–158.
- [21] Fitzgerald KA, McWhirter SM, Faia KL, et al. IKKε and TBK1 are essential components of the IRF3 signaling pathway. *Nat Immunol.* 2003;4:491–496.
- [22] Li G, Liu X, Yang M, et al. Crystal structure of African swine fever virus pS273R protease and implications for inhibitor design. *J Virol.* 2020;94(10). DOI:10.1128/JVI.02125-19
- [23] Xie P, Peng Z, Chen Y, et al. Neddylation of PTEN regulates its nuclear import and promotes tumor development. *Cell Res.* 2021;31:291–311.
- [24] Huang J, Xie P, Dong Y, et al. Inhibition of Drp1 SUMOylation by ALR protects the liver from ischemia-reperfusion injury. *Cell Death Differ.* 2021;28:1174–1192.
- [25] Renner F, Moreno R, Schmitz ML. Sumoylation-Dependent localization of IKKε in PML nuclear bodies is essential for protection against DNA-damage-triggered cell death. *Mol Cell.* 2010;37:503–515.
- [26] Reis AL, Netherton C, Dixon LK. Unraveling the armor of a killer: evasion of host defenses by African swine fever virus. *J Virol.* 2017;91. DOI:10.1128/JVI.02338-16
- [27] Dixon LK, Islam M, Nash R, et al. African swine fever virus evasion of host defences. *Virus Res.* 2019;266:25–33.
- [28] Li S, Yang J, Zhu Y, et al. Chicken DNA sensing cGAS-STING signal pathway mediates broad spectrum antiviral functions. *Vaccines (Basel).* 2020;8:369.
- [29] Paz S, Sun Q, Nakhaei P, et al. Induction of IRF-3 and IRF-7 phosphorylation following activation of the RIG-I pathway. *Cell Mol Biol (Noisy-le-Grand).* 2006;52:17–28.
- [30] Gatot J-S, Gioia R, Chau T-L, et al. Lipopolysaccharide-Mediated interferon regulatory factor activation involves TBK1-IKKε-dependent Lys63-linked polyubiquitination and phosphorylation of TANK/I-TRAF. *J Biol Chem.* 2007;282:31131–31146.
- [31] Balka KR, Louis C, Saunders TL, et al. TBK1 and IKKε act redundantly to mediate STING-induced NF-κB responses in myeloid cells. *Cell Rep.* 2020;31:107492.
- [32] Dubrau D, Tortorici MA, Rey FA, et al. A positive-strand RNA virus uses alternative protein-protein interactions within a viral protease/cofactor complex to switch between RNA replication and virion morphogenesis. *PLoS Pathog.* 2017;13:e1006134.
- [33] Hickey CM, Wilson NR, Hochstrasser M. Function and regulation of SUMO proteases. *Nat Rev Mol Cell Biol.* 2012;13:755–766.
- [34] Mukhopadhyay D, Dasso M. Modification in reverse: the SUMO proteases. *Trends Biochem Sci.* 2007;32:286–295.
- [35] Ding J, McGrath WJ, Sweet RM, et al. Crystal structure of the human adenovirus proteinase with its 11 amino acid cofactor. *Embo J.* 1996;15:1778–1783.
- [36] de Wit E, van Doremalen N, Falzarano D, et al. SARS and MERS: recent insights into emerging coronaviruses. *Nat Rev Microbiol.* 2016;14:523–534.
- [37] Mielech AM, Chen Y, Mesecar AD, et al. Nidovirus papain-like proteases: multifunctional enzymes with

- protease, deubiquitinating and deisgylating activities. *Virus Res.* [2014](#);194:184–190.
- [38] Shin D, Mukherjee R, Grewe D, et al. Papain-like protease regulates SARS-CoV-2 viral spread and innate immunity. *Nature.* [2020](#);587:657–662.
- [39] Netherton CL, Wileman TE. African swine fever virus organelle rearrangements. *Virus Res.* [2013](#);173:76–86.
- [40] Zhao G, Li T, Liu X, et al. African swine fever virus cysteine protease pS273R inhibits pyroptosis by noncanonically cleaving gasdermin D. *J Biol Chem.* [2022](#);298:101480.